CI&CEQ
Chemical Industry & Chemical Engineering Quarterly
Available on line at
Association of the Chemical Engineers of Serbia AChE
www.ache.org.rs/CICEQ
Chem. Ind. Chem. Eng. Q. 21 (4) 527–536 (2015) CI&CEQ

VESNA S. CVETKOVIĆ[1]
LUKA J. BJELICA[2]
NATAŠA M. VUKIĆEVIĆ[1]
JOVAN N. JOVIĆEVIĆ[1]

[1]Institute of Chemistry, Technology and Metallurgy, University of Belgrade, Belgrade, Serbia
[2]Faculty of Sciences and Mathematics, University of Novi Sad, Novi Sad, Serbia

SCIENTIFIC PAPER

UDC 544.6:669.729:543.42

DOI 10.2298/CICEQ141205009C

ALLOY FORMATION BY Mg UNDER-POTENTIAL DEPOSITION ON Al FROM NITRATE MELTS

Article Highlights

- Water removal from magnesium nitrate hexahydrate
- Preparation of magnesium nitrate melts
- Underpotential deposition of magnesium on aluminium substrate
- Mg-Al surface alloy formation by UPD of magnesium

Abstract

Magnesium was underpotentially deposited on aluminium electrodes from magnesium nitrate-ammonium nitrate melts at temperatures ranging from 390 to 500 K. The electrochemical techniques used were linear sweep voltammetry and potential step. Electrodes were studied by scanning electron microscopy (SEM), energy dispersive spectrometry (EDS), energy dispersive X-ray spectroscopy (EDX) and X-ray diffraction (XRD). It was found that reduction processes of nitrate, nitrite and water (when present), in the underpotential range studied, took part simultaneously with magnesium underpotential deposition. Consequently, magnesium UPD reduction and stripping voltammetry peaks were not pronounced and well defined. Nevertheless, EDS, EDX and XRD measurements showed evidence of Mg_2Al_3, $MgAl_2$ and $Al_{12}Mg_{17}$ alloys formed by underpotential deposition of magnesium onto aluminium substrate.

Keywords: magnesium/aluminium alloys, underpotential deposition, magnesium nitrate melts.

One of the ways to obtain a metal, and/or an alloy, under very controlled conditions is direct isothermal electrochemical deposition (electrodeposition). The current density that sustains electrochemical deposition of a metal, or an alloy, directly reflects the rate of the process [1].

However, metals like Li, Na, K, Al, Mg, Ti and W cannot be electrodeposited from water solutions, because hydrogen starts evolving on the working cathode before any of them start depositing. This prevents even the smallest amounts of the metal from remaining as a deposit on an electrode in a water solution without being dissolved. For electrodeposition of Al, Mg and other metals, with very negative standard electrode potentials, melts based on chloride salts at temperatures above 900 K are used. These are mainly inorganic or organic, chlorides or fluorides, salts that are combined with a cation of some alkaline/alkaline earth metal, or some organic cation or anion [1-3]. Ionic liquids (made of organic salts) became known relatively recently and proved to be suitable media for electrodeposition of metals and alloys at relatively low temperatures (from 273 to 373 K) [1,4].

To electrodeposit bulk of any metal, it is necessary to provide a working electrode with a potential that is more negative than the standard electrode potential of the depositing metal, this process is referred to as overpotential deposition (OPD). It was also found that it is possible to co-deposit two or even three metals using overpotential deposition conditions and thus produce alloys on the surface of the working electrode.

Further detailed investigations of the processes that regulate electrodeposition of metals and alloys lead to the recognition of electrodeposition of metals on foreign substrates at potentials more positive than

Correspondence: V.S. Cvetković, Institute of Chemistry, Technology and Metallurgy, University of Belgrade, Njegoševa 12,11000 Belgrade.
E-mail: v.cvetkovic@ihtm.bg.ac.rs
Paper received: 5 December, 2014
Paper revised: 26 February, 2015
Paper accepted: 20 March, 2015

the equilibrium potential of the depositing metal (also referred to as underpotential deposition – UPD) [5]. In the last 40 years, UPD has been a subject of intensive experimental and theoretical interest. Most of the initial experimental work was done in aqueous electrolytes until the 1980s when the same phenomena was observed in deposition experiments of aluminium on gold, silver and copper from chloride melts at temperatures below 573 K [6-8].

It was soon found that a metal electrodeposited under UPD conditions from aqueous, non-aqueous solutions and melts at room temperatures onto a cathode of a different metal can diffuse into the substrate and generate alloys. Alloys obtained by electrochemical deposition (OPD and UPD) can have different chemical and phase structures than the alloys of the same composition obtained by metallurgical (thermal) methods [1,9].

Over the past ten years, the automotive industry has shown renewed interest in the applications of magnesium and its alloys, because magnesium with a density of 1.74 g/cm^3 is 4.5 times lighter than steel and 1.6 times lighter than aluminium [10,11], while being able to achieve similar levels of ultimate strength in some alloys (200-250 MPa). As a result, magnesium alloys offer a very high specific strength among conventional engineering alloys and have a wide application prospect in aerospace transportation, electronic engineering, as well as electrode components as chemical sources of electrical energy [12,13]. Currently, the most widely used magnesium alloys are based on the Mg-Al system [12]. Electrodeposition of magnesium and its alloys is of increasing importance in the development of rechargeable magnesium battery systems [14].

It is known that Mg cannot be deposited from solutions of simple Mg salts such as $Mg(ClO_4)_4$ in conventional organic solvents, for example, acetonitrile, propylene carbonate or dimethylformamide. Most likely, this is due to the working electrode surface becoming covered by passivating surface films of very low ionic conductivity [14].

Available literature that references electrodeposition of magnesium from nitrate melts, and magnesium underpotential deposition is rather limited, while that of alloy formation from nitrate melts is practically nonexistent. Physicochemical characteristics of nitrate melts of alkaline and alkaline earth metals became a subject of interest in the second half of twentieth century [15-17] including their possible usage as electrolytes [18-20]. However, among a number of nitrate melts investigated electrochemically, neither magnesium nitrate nor magnesium nitrate-ammonium nitrate mixture melts were studied.

There are multiple reasons why these melts are not conducive to this work. Very pronounced oxidative characteristics of nitrates, great number of oxidation/ /reduction processes that can take place with cations and anions present in nitrates at the potentials more negative and more positive than the reversible potential of magnesium [19,20], prevent realization of more experiments regarding metal electrodeposition from nitrate melts. Difficulties related to sustaining of the intended melt temperature variation below ±3 K arise from the large latent heats of the numerous nitrates, phase transformations in the temperature range from 373 to 500 K [15]. Also, it is impossible to remove water from magnesium nitrate hexahydrate by heating, because it decomposes before it loses water and transforms into magnesium(II) oxide. The backbone of this octahedral complex is the magnesium cation $[Mg(H_2O)_6]^{2+}$, which is very stable and cannot lose water thermally. As such, presence of water in magnesium melts cancels the advantages the melts have as compared to the magnesium aqueous solutions.

The aim of this work was to overcome the limitations of working on electrodeposition from nitrate melts, establish whether underpotential deposition of magnesium onto aluminium surface from magnesium nitrate melts occurred, and if it lead to magnesium/ aluminium alloy formation.

EXPERIMENTAL

Experiments were done under 99.99% Ar atmosphere in a three-neck (joints) electrochemical cell made of Pyrex glass placed in a heating mantle with temperature controlled (electronic thermostat) between 363 and 463 (±2 K). The central neck was closed with a PTFE plug carrying the working electrode (a 99.999% Al plate with active surface area of 0.4 cm^2), the left neck with a PTFE plug holding an argon glass inlet-outlet and glass Luggin capillary with magnesium reference electrode (3 mm diameter 99.999% Mg wire), and the right neck with a Teflon plug holding a magnesium anode (99.999% Mg) in the shape of a curved rectangular shovel (7.5 cm^2 active surface area) and a tube of thin glass with a thermocouple. Argon and other possible gases coming out of the cell were captured/washed in two bottles (first with a slightly basic solution and second with a slightly acid solution). The entire cell setup was placed into a transparent plastic “glove box” in order to create a moisture free atmosphere around the cell.

The melts used in experiments were: non-aqueous $Mg(NO_3)_2$, $Mg(NO_3)_2{\cdot}XH_2O$, eutectic mixture non-aqueous $Mg(NO_3)_2$: NH_4NO_3 and eutectic mixture $Mg(NO_3)_2{\cdot}6H_2O + NH_4NO_3{\cdot}xH_2O$.

The procedure for water removal from magnesium nitrate hexahydrate consisted of two steps. The first step: the mixture of 5 g of magnesium nitrate hexahydrate and 15 cm^3 of trimethyl orthoformate was brought to boiling and kept for 90 min under reflux at 343 K. In the first 20 min $Mg(NO_3)_2{\cdot}6H_2O$ was completely dissolved in trimethyl orthoformate and after 45 min snow white crystals started appearing at the walls of the glass vessel. The second step: after 90 minutes of previous treatment, the mixture, now consisting of an ethyl ester of formic acid, methanol and crystals of non-aqueous magnesium nitrate, was subjected to vacuum distillation at 343 K. Upon removal of the visible liquid, the remaining crystals were vacuum dried for additional 60 min. Non-aqueous magnesium nitrate was kept in a closed glass container in a desiccator furnished with plenty of silicagel. Ammonium nitrate hexahydrate was dried for 10 h at 378 K. Required amounts of magnesium nitrate alone, or mixtures with ammonium nitrate, were placed into the cell supplied with electrodes. Closed cell was then placed into the heating mantel, argon supply was turned on and the system was heated gradually to the wanted temperature.

The aluminium cathodes (99.999% Al) were mechanically polished by emery paper (FEPA P-4000) to a mirror finish and then etched in (50% HF + 15% H_2O_2) water solution for 30-60 s with intensive steering before being left in (NH_4NO_3 + 5% H_2O_2) solution for 30-60 s. Finally, the electrodes were washed in deionised water, absolute ethyl alcohol, dried and mounted into the cell.

The magnesium anode and reference electrode (99.999% Mg) were mechanically polished by emery paper (FEPA P-4000) to a mirror finish and then etched in the solution, made of 78.2 cm^3 conc. HNO_3 + 23.4 cm^3 conc. H_2SO_4 + 898.4 cm^3 deionised water, in several 10 s intervals alternating with washing with deionised water. Finally, the electrodes were washed in deionised water, absolute ethyl alcohol, dried and mounted into the cell.

The electrochemical techniques used were: linear sweep voltammetry (LSV) and potential step. The potentials of working electrodes were measured in relation to the equilibrium potential of magnesium reference electrode in the melt used under the given conditions.

The cyclic voltammetry experiments included one or more cycles of the working electrode potential cycling from a starting potential, E_S (usually 50 to 100 mV more negative than the reversible potential of the Al working electrode) to a final potential, E_F (which was positive to the reversible potential of Mg) and then back again to E_S all at scan rates (between 5 and 100 mVs^{-1}). The obtained results were recorded on an *X-Y* recorder.

The potential step method included change of the working electrode potential from an initial potential, E_I (50 to 100 mV more negative to aluminium equilibrium potential in the given melt) to a potential, E_X (50 to 100 mV more positive to magnesium equilibrium potential in the given melt). E_X potential was held constant for some time, whereupon the cathode was retrieved from the cell under potential in order to preserve deposited material or possible alloys formed during UPD of magnesium. The electrodes were successively washed with deionised water and absolute ethyl alcohol until visible remains of melt were removed. The surfaces of the electrodes were analyzed by scanning electron microscopy (SEM - JEOL, model JSM-5800, Japan), energy dispersive spectrometry (EDS - Oxford INCA 3.2, U.K.), energy dispersive X-ray spectroscopy (EDX-maping - Oxford IncaEnergy EDX) and X- ray diffraction (XRD - Enraf Nonius powder diffractometer, Germany). IR analysis of the "anhydrous" magnesium nitrate was performed using Thermoscientific Nicolet 6700 (FT-IR) Smart Orbit Diamond (4000-200 cm^{-1}).

RESULTS AND DISCUSSION

It was important to make sure that the method of water removal from magnesium nitrate described above is effective. The mass difference between the magnesium nitrate hexahydrate entering the process of water removal and the magnesium nitrate leaving the said process was 39±3%. This would suggest that at least 92% of water had been removed. The difference to 100% can be attributed to the residual methanol, methyl ester of formic acid or some of their derivatives because obtained $Mg(NO_3)_2$ crystals appeared to give off these chemicals immediately after drying. Obtained results strongly suggest that the process of water removing from magnesium nitrate hexahydrate was successful. This conclusion is supported by the results obtained with IR and XRD analysis (Figures 1 and 2). The results of "anhydrous" magnesium nitrate IR analysis (Figure 1) show [21,22]: a) OH group at 3235 cm^{-1}; b) CH groups at 2960 and 2850 cm^{-1}; c) NO_3 at 1344, 1128 and 1012 cm^{-1}, possibly MgO group at 644 and 407 cm^{-1} and support the above conclusions.

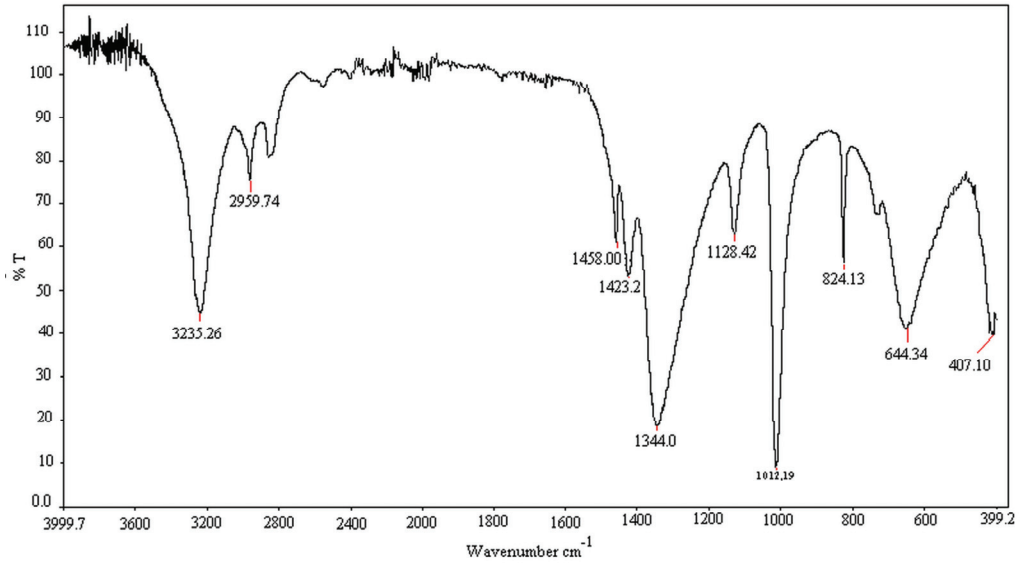

Figure 1. IR spectrogram of $Mg(NO_3)_2$ crystals obtained after water removing process.

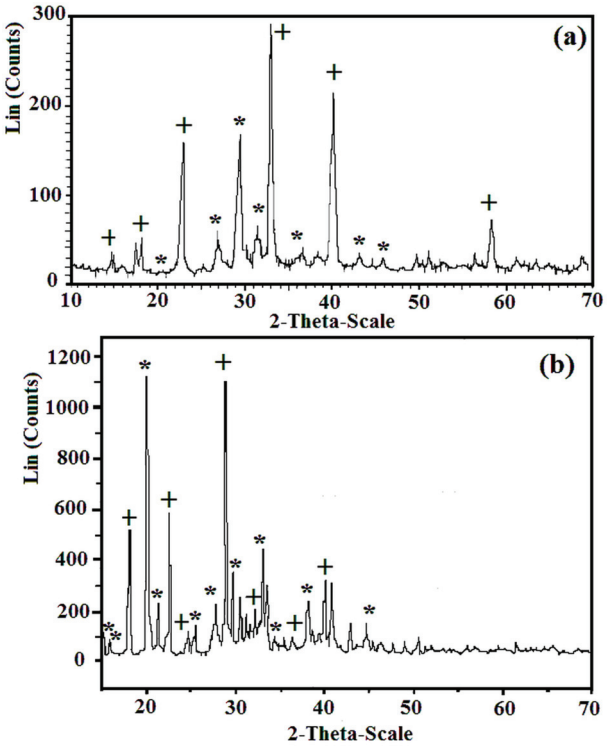

Figure 2. XRD spectra of: a) non-aqueous eutectic mixture $Mg(NO_3)_2$ + NH_4NO_3, (*) $Mg(NO_3)_2$, (+) NH_4NO_3; b) eutectic mixture $Mg(NO_3)_2{\cdot}6H_2O$ + $NH_4NO_3{\cdot}xH_2O$; (*) $Mg(NO_3)_2{\cdot}6H_2O$, (+) $NH_4NO_3{\cdot}XH_2O$ [24,25].

In Figure 2a, XRD measurements do not show characteristic lines which would belong to the crystal structure of $Mg(NO_3)_2{\cdot}6H_2O$ shown in Figure 2b. They show the lines, which with some reservations could be attributed to the crystals of "anhydrous" magnesium nitrate. The reservations are due to the fact that the data on "anhydrous" magnesium nitrate in the available literature are very few and not fully reliable.

Contrary to work solutions where hydrogen ions are present and where hydrogen reference electrode can be universal, there is no universal reference electrode in experiments with melts. Therefore, in the systems where underpotential deposition is examined it is common practice to use the reversible potential of the depositing metal as a reference electrode potential with ascribed value of 0.000 V. In the nitrate melts used, for magnesium underpotential deposition on aluminium, a magnesium electrode was used as the reference electrode. Polarization measurements and cyclic voltammetry performed on the magnesium working electrode with magnesium reference and counter electrodes have shown that magnesium reversible potential in the used magnesium nitrate melts, under temperatures ranging from 340 to 500 K, was stable [23]. Reversible potential of polycrystalline aluminium in anhydrous $Mg(NO_3)_2$ melt at temperature interval between 360 and 400 K was 630±10 mV *vs.* Mg/Mg(II); in non-aqueous eutectic mixture $Mg(NO_3)_2$ + NH_4NO_3 at temperature between 390 and 500 K was 970±20 mV *vs.* Mg/Mg(II); in $Mg(NO_3)_2{\cdot}6H_2O$ melt between 440 and 500 K was 260±30 mV *vs.* Mg/Mg(II) and in eutectic mixture $Mg(NO_3)_2{\cdot}6H_2O$ + $NH_4NO_3{\cdot}xXH_2O$ at temperature interval between 380 and 450 K was 1000±30 mV *vs.* Mg/Mg(II). With all other conditions being kept constant, the higher the temperature, the more positive aluminium reversible potential is. Addition of ammonium nitrate to magnesium nitrate moved the aluminium reversible potential to more positive values as well.

General characteristics of the voltammograms obtained in all melts used is that more than one reduction peak was observed in the magnesium underpotential area, but with no oxidation counterparts. Typical example of the voltammograms obtained is presented in Figure 3. It can be seen that stripping peaks were not observed even when the cathodic end potential was pushed into the overpotential range. Sometimes reduction peaks were spread over a wider range of applied potentials without showing a steeper increase or decrease of current density values. Such structures of voltammogram peaks are characteristic for processes that start at close successive potentials and proceed simultaneously (often next process starts and increases rate while previous process dyes out with falling rate). Therefore, the obtained peaks represent a sum of all the rates of all the processes taking part at the certain potential.

Suggestions of possible processes that could produce reduction peaks in the magnesium UPD region investigated, apart from ones brought about by the magnesium underpotential deposition itself, can be found in rare published works [19,20]. The potentials of the proposed reactions measured relative to Na, K or Li cannot be directly used, but it can be assumed with enough certainty that the order of the potentials and their differences between these processes is preserved with respect to the magnesium reference potential. However, absolute values must be changed by the amounts that reflect differences in reference potentials between Na, K and Li in their nitrate melts and magnesium in used nitrate melts.

Reduction processes in the nitrate melts with water present, at the most anodic potentials, start with:

$$2NO_3^- + 6H_2O + 10e^- \rightleftharpoons N_2 + 12OH^- \quad (1)$$

$$NO_3^- + H_2O + 2e^- \rightleftharpoons NO_2^- + 2OH^- \quad (2)$$

followed by the group of reactions with very close nitrate reduction potentials, in the melts with and without water present, which is reflected in wider cathodic voltammogram peaks:

$$NO_3^- + 5e^- \rightleftharpoons 1/2N_2 + 3O^{2-} \quad (3)$$

$$NO_3^- + 2e^- \leftrightarrow NO_2^- + O^{2-} \quad (4)$$

$$2NO_3^- + 2e^- \leftrightarrow 2NO_2^- + O_2^{2-} \quad (5)$$

$$2NO_3^- + 8e^- \leftrightarrow N_2O + 5O^{2-} \quad (6)$$

$$NO_3^- + 3e^- \rightleftharpoons NO + 2O^{2-} \quad (7)$$

which at their end decrease close to zero cathodic current densities. At potentials of -350 to -600 mV more negative to the previous peak, but still in the magnesium UPD region, next group of the nitrate reduction processes starts at mutually very close potentials:

$$2NO_3^- + 2e^- \rightleftharpoons 2NO_2^- + O_2^{2-} \quad (8)$$

$$NO_3^- + e^- \rightleftharpoons NO_2 + O^{2-} \quad (9)$$

The absence of anodic (oxidation) counterparts to the cathodic peaks was a subject of a number of works [9,19,20,26-28]. These studies emphasize that changes of the aluminium electrode potential in nitrate melts from anodic to cathodic values compared to magnesium reversible potential provoke passivation of the working electrode which becomes partially (or fully) covered with magnesium oxides layers. These layers do not dissolve when the potential is returned to the starting positive value.

In the UP region of the magnesium on aluminium cycle in nitrate melts used, the change of the electrode potential from positive values up to the

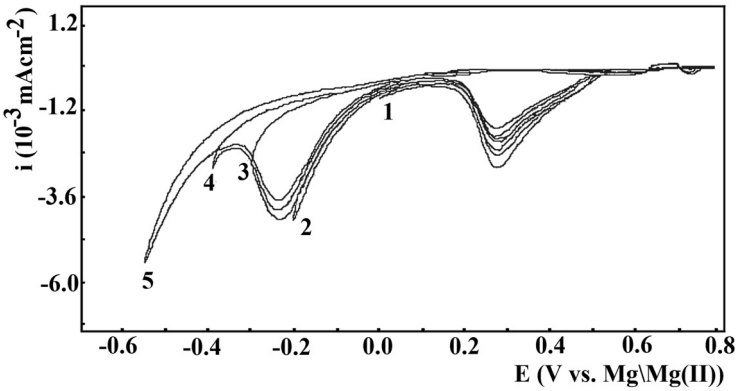

Figure 3. Linear sweep voltammograms of magnesium deposition onto aluminium electrode, υ = 30 mV s^{-1} from non-aqueous eutectic mixture $Mg(NO_3)_2$ + NH_4NO_3 at T = 430 K, E_i = 0.700 V ↔ E_f = -0.550 V vs. Mg/Mg(II).

magnesium reversible potential induces a number of reactions based on nitrogen, very reactive oxygen anion O^{2-}, OH^- and sometimes water. All produced gases were removed from the electrochemical cell by the argon stream, so when the electrode potential is reversed into positive direction, their possible theoretical reverse oxidation reaction back to initial NO_3^- or H_2O could not be expected. As a result, no anodic voltammogram peaks could be recorded. Furthermore, O^{2-} produced in inner and outer parts of the electrochemical double layer very quickly engaged in reaction with present Mg^{2+} [9,19,20,26-28]:

$$Mg^{2+} + O^{2-} \rightarrow MgO \quad (10)$$

the result being formation of insoluble magnesium oxides in the magnesium UPD region. The thermal decomposition constant [19,20] defines the stability of the possibly present magnesium hydroxide:

$$Mg(OH)_2 \rightleftharpoons MgO + H_2O \quad (11)$$

However, examined anodic voltammogram peaks cannot be expected in the UP region.

In the melt made of eutectic mixture of magnesium nitrate and ammonium nitrate, at the temperatures used, ammonium ion, resulting from NH_4NO_3 dissociation [19,20], form the compound $(NH_4)_3Mg(NO_3)_5$. In the melt this compound exists as a quasicrystalline structure made of NH_4^+, Mg^{2+} and NO_3^- [19,20]. The fact that reduction current densities in the magnesium nitrate melts increase with the increase of the ammonium nitrate present, at the constant temperature in the magnesium UP region investigated, leads to the conclusion that NH_4^+ reduction is taking place:

$$2NH_4^+ + 2e^- \rightarrow 2NH_3 + H_2 \quad (12)$$

However, this reaction is, under given conditions, irreversible and voltammograms could not show oxidation peaks when the electrode potential was reversed in the positive direction.

It is logical to assume that the reduction peaks obtained by LSV measurements on the aluminium working electrode from magnesium nitrate and magnesium nitrate + ammonium nitrate melts in the magnesium underpotential region are sums of partial current densities for: Mg^{2+} underpotential reduction, nitrate anion reduction and ammonium cation reduction. Being a sum, the recorded current densities suggest small magnesium underpotential deposition partial current densities. Such small current densities exhibited by the UPD voltammograms from similar melts [9,23,29,30] were characteristic of deposited metal monolayer diffusion into the substrate and forming alloys.

According to the Hume/Rothery rules [31], Mg and Al fulfil the required conditions to form alloys (solid solutions), including "the 15% rule", because Mg and Al atomic radii differ only by 16.6%. EDS and XRD measurements obtained from the aluminium electrodes in used magnesium nitrate melts exposed to constant potentials in the magnesium underpotential region (50 to 150 mV *vs.* Mg/Mg(II)) supported the assumption.

An example of the indication that magnesium does underpotentially deposit on aluminium is exhibited in Figure 4 and represents SEM, EDS and EDX

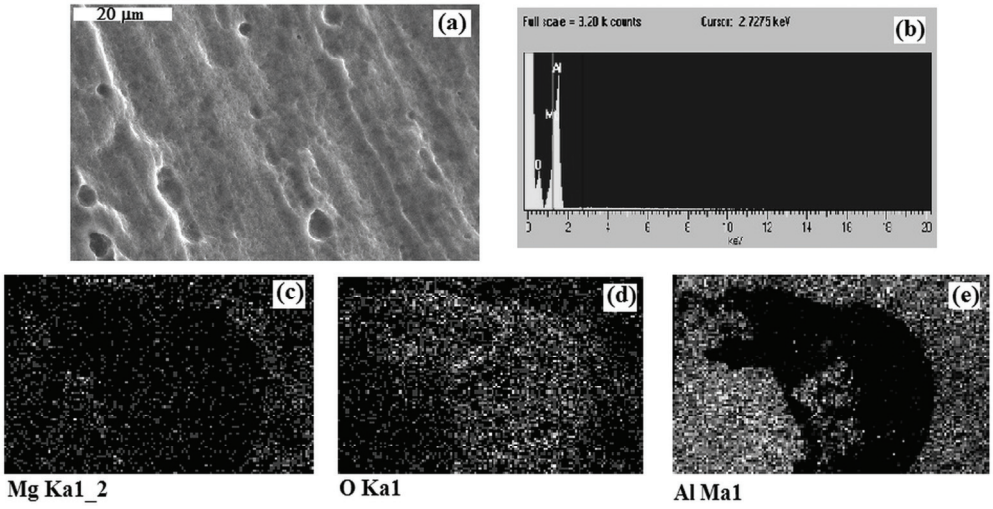

Figure 4. a) SEM photograph for the surface of the Al electrode after 120 min holding at the potential of E_x = 60 mV vs. Mg/Mg(II) in non-aqueous eutectic mixture $Mg(NO_3)_2$ + NH_4NO_3 at T = 450 K, mag. 2500x; b) EDS data for the sample in Figure 4a and EDX mapping; c) magnesium distribution image; d) oxygen distribution image; and e) aluminium distribution image of the Al electrode surface.

results obtained from the aluminium electrode held for two hours at magnesium underpotential of 60 mV *vs.* Mg/Mg(II) in a non-aqueous eutectic mixture $Mg(NO_3)_2$ + NH_4NO_3 at T = 450 K. A typical example of XRD analysis results on the aluminium sample exposed to underpotential of 60 mV *vs*. Mg/Mg(II) in the same melt and at T = 460 K for: a)1, b) 2 and c) 5 h are shown in Figures 5a-c, and strongly suggest that magnesium-aluminium alloys are being formed.

The results obtained by EDS, EDX (Table 1) and XRD (Table 2) analysis of Al substrates after being exposed to magnesium underpotential deposition to constant potential of 60 to 100 mV *vs.* Mg/Mg(II) for 120 min, from all used melts at the temperatures applied (under 500 K) seriously indicate that magnesium-aluminium alloys have been formed.

Table 1. Results of EDS quasi-quantitative analysis for the Al samples exposed to constant potential of 60 to 100 mV vs. Mg/Mg(II) for 120 min in used melts

Melt	Al (at.%)	Mg (at.%)	O (mass%)
$Mg(NO_3)_2{\cdot}6H_2O$	-	-	-
$Mg(NO_3)_2$	59.99	6.22	33.79
$Mg(NO_3)_2{\cdot}6H_2O$ + $NH_4NO_3{\cdot}xH_2O$	94.63	5.37	-
$Mg(NO_3)_2$ + NH_4NO_3	19.19	11.45	69.37

According to the Mg-Al phase diagrams [36,37], the equilibrium solid phases are: a) the fcc solid solution with maximum solubility Mg in Al of at.18.9% at eutectic temperature of 723 K; b) the hcp solid solution with maximum solubility of Al in Mg of 11.8 at.% at eutectic temperature of 710 K; c) the β compound of approximate stoichiometry Al_3Mg_2, with complex fcc structure at low temperature, β transforms martensitically to another structure that may be a distortion of the β structure, but the equilibrium phase relations have not been investigated); d) the line compound R (or ε), of composition 42 at.% Mg; e) compound γ which at 723 K has a maximum composition range of approximately 45-60 at.% Mg, but the ideal crystal structure has the stoichiometry $Al_{12}Mg_{17}$ at 58.6 at.% Mg. At the lower cooling rates, β, γ and γ' can be formed, while at higher cooling rates a new phase Φ was observed, found in a 30 at.% Mg alloy where a metastable solid solution and metastable phase appeared. Based on the structure, the new phase was identified as having stoichiometry Al_2Mg.

All of the alloys described by the literature [36,37] have been recorded in magnesium underpotential deposition performed on aluminium in used nitrate melts but at temperatures that are several hundred K lower, Table 2. There is β compound (Al_3Mg_2) with complex fcc structure which is known to exist over a range of composition. This compound starts as a supersaturated Al solid solutions and

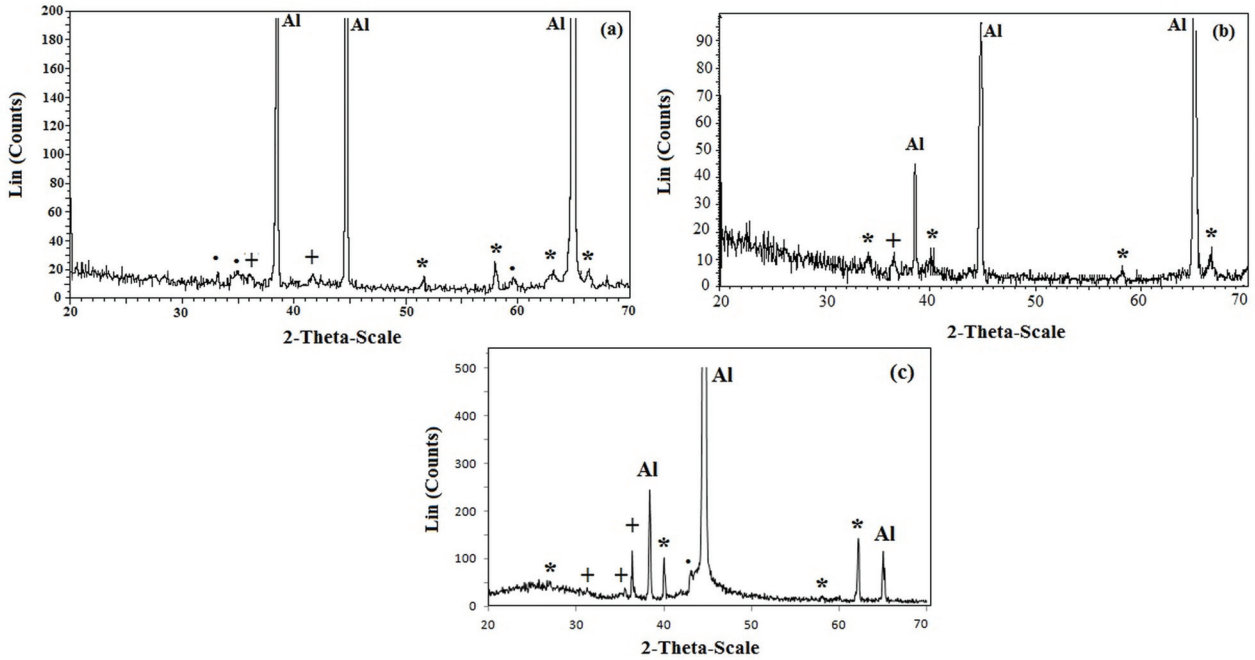

Figure 5. Diffraction patterns of aluminium sample after: a) 1, b) 2 and c) 5 h of magnesium underpotential deposition at E_x = 60 mV vs. Mg/Mg(II) in non-aqueous eutectic mixture $Mg(NO_3)_2$ + NH_4NO_3 at T = 460 K; a) (·) (hcp) - $Al_{0.9}Mg_{3.1}$[32]; (*) (bcc) - $Al_{12}Mg_{17}$[33]; (+) (hcp) - Mg_2Al_3 [34]; b) (+) (hcp) - Mg_2Al_3 [34]; (*) (bcc) - $Al_{12}Mg_{17}$[33]; c) (+) (hcp) - Mg_2Al_3 [34]; (*) (bcc) - $Al_{12}Mg_{17}$[33]; (·) - (rhombohedral) MgO_4 [35].

undergoes a phase transformation through continued decomposition by formation of a nonequilibrium phase β' and solid solution with less Mg content than equilibrium, and ends up in the formation of equilibrium β phase. The metastable solid solution with relatively high Mg content (up to 30 at.%) with approximate stoichiometry Al_2Mg was also recorded. The apparent existence of $Al_{12}Mg_{17}$ (at 58.6 at.% Mg) is a rather convincing argument in support of very successful interdiffusion of Mg and Al during magnesium underpotential deposition onto aluminium performed here at temperatures ranging from 390 to 500 K.

Table 2. Alloys identified by XRD analysis on Al substrates exposed to constant potential of 60 to 100 mV vs. Mg/Mg(II) (magnesium UPD) for 120 min in used melts

Melt	Alloy 1	Alloy 2
$Mg(NO_3)_2{\cdot}6H_2O$	bcc - $Al_{12}Mg_{17}$	
$Mg(NO_3)_2$	bcc - $Al_{12}Mg_{17}$	fcc - Al_3Mg_2
$Mg(NO_3)_2{\cdot}6H_2O + NH_4NO_3{\cdot}xH_2O$	fcc - Al_2Mg	hcp - Mg_2Al_3
$Mg(NO_3)_2 + NH_4NO_3$	bcc - $Al_{12}Mg_{17}$	hcp - Mg_2Al_3

Which of the magnesium adatoms formed by underpotential deposition on aluminium surface participate in oxide formation and which ones diffuse into substrate and contribute to alloy formation could not be concluded by linear sweep voltammetry, EDS or XRD results. LSV results indicated, EDS and XRD results confirmed, formation of both the magnesium oxide and the magnesium-aluminium alloy at the surface of the aluminium electrode in nitrate melts used. Eqs. (3)–(9) describe sources of oxygen needed for the process shown in Eq. (10) in the absence of water and Eq. (11) magnesium oxide formation in the presence of water in the melt. In addition, some novel results [26-28] suggest that every amount of reactive magnesium on the electrode surface in the presence of O^{2-} and OH^- very quickly becomes MgO. Therefore, the surface of the aluminium working electrode becomes partially covered with MgO_x even in the first linear change of the potential from anodic end to cathodic end of the magnesium underpotential range. This, however, did not preclude enough of magnesium adatoms from participating in magnesium-aluminium alloys formation by interdiffusion. Part of the magnesium ions in magnesium (II) oxide probably diffuse through the oxide layer to the aluminium surface where they become discharged into magnesium adatoms which are then participating in the interdiffusion processes. Fast and unavoidable formation of insoluble MgO in the magnesium underpotential deposition range on aluminium from used nitrate melts explains quasi-passivation of the working electrode and the lack of anodic current peaks on the voltammograms recorded.

CONCLUSIONS

The value for the half of work function difference in the case of Al and Mg is 0.20 to 0.30 eV and magnesium should show an underpotential deposition on aluminium at potentials close to 0.100 V *vs.* Mg/Mg(II). This work has confirmed UPD of Mg on Al substrate from nitrate melts used at potentials very close to 100 mV *vs*. Mg/Mg(II).

However, this rule does not predict whether there are going to be alloys formed between the substrate and underpotentially deposited metal. And yet, the most pronounced effects of the established magnesium underpotential deposition from magnesium nitrate melts used were three alloys formed with aluminium substrate: $Al_{12}Mg_{17}$, Mg_2Al_3 and metastable solid solution Al_2Mg. All the alloys obtained were formed at the temperatures several hundred Kelvin degrees lower than the temperatures which are, according to the relevant existing binary phase diagrams, needed for their formation thermally.

It was established that underpotential deposition of the metals unsuitable for electrodeposition from aqueous electrolytes, like magnesium, can be performed even from low temperature nitrate melts and that it can lead to the formation of alloys in a very controlled way under more technologically suitable conditions than most of the known ones.

Acknowledgement

This work was supported by the Ministry of Education, Science and Technological Development of the Republic of Serbia (Grant ON 172060).

REFERENCES

[1] D.M. Kolb, in Advances in electrochemical science and engineering, Vol. 7, R.C. Alkire, D.M. Kolb, Eds., Wiley-VCH, Weinheim, 2001, p. 150

[2] A.M. Martinez, G.M. Haarberg, B. Borresen, Y. Castrillejo, R. Tunold, J. Appl. Electrochem. **34** (2004) 1271-1278

[3] Z. Lu, A. Schechter, M. Moshkovich, D. Aurbach, J. Electroanal. Chem. **466** (1999) 203-208

[4] G. Mamantov, C.L. Hussey, R. Marassi, in: Techniques for characterisation of electrodes and electrochemical processes, R. Varma, J.R. Selamn, Eds., John Wiley and Sons, New York, 1991, p. 471

[5] D.M., Kolb, M. Przasnyski, H. Gerischer, J. Electroanal. Chem. **54** (1974) 25-38

[6] B.S. Radović, R.A.H. Edwards, J.N. Jovićević, J. Electroanal. Chem. **428** (1997) 113-121

[7] B.S. Radović, V.S. Cvetković, R.A.H. Edwards, J.N. Jovićević, Kovove Mater. **48** (2010) 159-171

[8] B.S. Radović, V.S. Cvetković, R.A.H. Edwards, J.N. Jovićević, Kovove Mater. **48** (2010) 55-71

[9] G.L. Stafford, C.L. Hussey, In Advances in Electrochemical Science and Engineering, Vol. 7, R.C. Alkire, D.M.Kolb, Eds., Wiley-VCH, Verlag GmbH, Weinhaim, 2002, p. 275

[10] L.L. Rokhlin, In Advances in Metallic alloys, Vol. 3, J.N. Fridlyander, D.G. Eskin, Eds., Taylor& Francis, New York, 2003, p. 1

[11] P.A. Friedman, W.B. Copple, JMEP **13** (2004) 335-347

[12] Z.H. Ye, X.Y. Liu, J. Mater. Sci. **39** (2004) 6153-6171

[13] D. Eliezer, E. Aghion, F. H. Froes, Adv. Perform. Mater. **5** (1998) 201-212

[14] Y. Viestfrid, M.D. Levi, Y. Gofer, D. Aurbach, J. Electroanal. Chem. **576** (2005) 183-195

[15] K.V. Ramana, R.C. Sharma, H.C. Gaur, J. Chem. Eng. Data **31** (1986) 288-291

[16] K.V. Ramana, R.C. Sharma, H.C. Gaur, J. Chem. Eng. Data **35** (1990) 293-301

[17] K.V. Ramana, R.C. Sharma, H.C. Gaur, J. Chem. Eng. Data **35** (1990) 418-420

[18] K. Bhatia, R.C. Sharma, H.C. Gaur, Electrochim. Acta **23** (1978) 1367-1369

[19] D.A. Tkalenko, Elektrokhimiya nitratnykh rasplavov, Naukova Dumka, Kiev, 1983

[20] D.A. Tkalenko, Makrokinetika katodnykh protsessov v gidroksidnykh i nitratnykh rasplavakh, Naukova Dumka, Kiev, 1993

[21] A.G. Adebayo, Y. Liang, R.C. Miranda, S. Scandolo, J. Chem. Phys. **131** (2009) 014506

[22] A.M. Hofmeister, E. Leppel, K.A. Speck, Mon. Not. R. Astron. Soc. **345** (2003) 16-38

[23] V.S. Cvetković, Underpotential Electrochemical deposition of magnesium from nitrate melts", Zadužbina Andrejević - PMF K. Mitrovica, Belgrade, 2012 (in Serbian)

[24] D. Weigel, B. Imelik, M. Prettre, Bull. Soc. Chim. Fr. (1964) 2600-2602

[25] R.J.Cernik, R. Delhez, E.J. Mittemeijer, Mater. Sci. Forum **359** (1996) 228-231

[26] N. Amir, O.V. Chusid, D.G. Aurbach, J. Power Sources **174** (2007) 1234-1240

[27] A.M. Martinez, B. Børrensen, G.M. Haarberg, Y. Catrillejo, R. Tunold, J. Electrochem. Soc. **151** (2004) C508

[28] A. Brenner, in Advances in electrochemistry and electrochemical engineering, C.W. Tobias, Ed., Interscience, New York, 1967, p.25

[29] B.S. Radović, V.S. Cvetković, R.A.H. Edwards, J.N. Jovićević, Int. J. Mater Res. **102** (2011) 59-68

[30] N. Jovićević, V.S. Cvetković, Ž.J. Kamberović, J.N. Jovićević, Metall. Mater. Trans., B **44** (2013) 106-114

[31] W. Hume-Rothery, R.E. Smallman, C.W. Haworth, The structure of metals and alloys, 5th ed., The Institute of metals, London, 1969

[32] H.L. Luo, C.C. Chao, P. Duwez, Trans. Met. Soc. AIME **230** (1964) 1488-1489

[33] C. Suryanarayana, Z. Metallkd. **69** (1978) 155-156

[34] B. Ribar, F. Gabela, R. Herak, B. Prelesnik, Z. Kristallogr. Kristallgeom. Kristalphys. Kristallchem. **137** (1973) 290--294

[35] V.M. Bakulina, S.A. Tokareva, E.I. Latysheva, J. Struct. Chem. **11** (1970) 150

[36] M. Hansen, K. Anderko, Constitution of binary alloys, McGraw-Hill, New York, 1958

[37] T.B. Massalski, Binary alloy phase diagrams, ASM, Metals Park, OH, 1990.

VESNA S. CVETKOVIĆ[1]
LUKA J. BJELICA[2]
NATAŠA M. VUKIĆEVIĆ[1]
JOVAN N. JOVIĆEVIĆ[1]

[1]Institut za hemiju, tehnologiju i metalurgiju, Centar za elektrohemiju, Univerzitet u Beogradu, Beograd, Srbija
[2]Prirodno-matematički fakultet, Univerzitet u Novom Sadu, Novi Sad, Srbija

NAUČNI RAD

FORMIRANJE LEGURA ELEKTROTALOŽENJEM Mg PRI POTPOTENCIJALIMA NA Al IZ RASTOPA NITRATA

Ispitivano je elektrotaloženje magnezijuma pri potpotencijalima (underpotential deposition - UPD) na elektrodi od aluminijuma iz rastopa smeše magnezijum nitrata i amonijum nitrata na temperaturama od 390 do 500 K. Elektrohemijske tehnike koje su korišćene bile su ciklička voltametrija i metoda potenciostatskog pulsa. Nakon elektrotaloženja magnezijuma pri potpotencijalima aluminijumske elektrode ispitivane su skenirajućom elektronskom mikroskopijom (SEM), energetsko disperzivnom spektroskopijom (EDS), energetsko disperzivnom spektroskopijom X-zraka (EDX) i metodom difrakcije X-zraka. Utvrđeno je da reakcije redukcije nitratnih i nitritnih jona i vode (kada je prisutna), koje se odigravaju u istom i širem području potpotencijala magnezijuma učestvuju istovremeno sa reakcijama elektrolitičkog taloženja magnezijuma u datom rastopu i deformišu i/ili prekrivaju redukcione struje elektrotaloženja magnezijuma. EDS, EDX i XRD merenja su pokazala da dolazi do formiranja Mg_2Al_3, $MgAl_2$ and $Al_{12}Mg_{17}$ legura kao posledice elektrotaloženja magnezijuma pri potpotencijalima na elektrodama od Al u ispitivanim rastopima.

Ključne reči: magnezijum/aluminijum legure, elektrotaloženje pri potpotencijalima, rastopi magnezijum-nitrata.